11th Australasian Fluid Mechanics Conference
University of Tasmania, Hobart, Australia
14-18 December 1992

DEFORMATION BEHAVIOUR OF LARGE POLYMERIC AND NEWTONIAN LIQUID BRIDGES IN STRETCHING (PLATEAU SIMULATION)

R. KROGER, S. BERG and H.J. RATH

ZARM, Centre of Applied Space Technology and Microgravity
University of Bremen, Hochschulring/ Am Fallturm
2800 Bremen 33, GERMANY

ABSTRACT

Large liquid bridges ($L_0 = 2R_0 = 50$ mm) placed between two equal plane circular disks have been stretched in a neutral buoyancy tank by moving one disk with a constant velocity. The contour of the deformed liquid bridge was measured and the velocity field within the bridge was detected by particle tracing. From the velocity field the local elongation rates were calculated. While surface tension forces minimize the surface area, leading to a contraction of the liquid bridge, friction forces due to shear and elongational viscosity act against it. Increasing viscosity tends to form more cylindrical bridges. The local elongation rates within the liquid bridges are not homogeneous. In cylindrical shaped bridges the difference between the highest and lowest local elongation rate is less than in strongly deformed low viscosity liquid bridges. The highest elongation rates occur in the middle of the bridge and are larger than the theoretical ones calculated for an ideal cylinder.

NOTATION

r, z	cylindrical coordinates
u	upper disk velocity
v_r, v_z	velocity components
$v_r(r,z)$, $v_z(r,z)$	velocity functions (Chebyshev)
Ca	Capillary number
L, L_0	liquid bridge length, initial length
R, R_0	liquid bridge radius, initial radius
R_c	ideal cylinder radius
R(z)	contour function
$\dot{\gamma}_{rr}$, $\dot{\gamma}_{zz}$	components of the rate-of-strain-tensor
$\dot{\epsilon}$	elongation rate
η_e, η_s or η	elongational, (zero) shear viscosity
σ	surface tension
τ_{rr}, τ_{zz}	components of the stress tensor
$\{..\}(z_0)$	average value in cross section $z = z_0$
$\{..\}_{max, min}$	maximun, minimum value in $0 \le z \le L$
$\{v_z\}_{rel}$	maximum flow velocity relativ to disk
$<..>$	overall average

INTRODUCTION

For the accurate determination of the elongational viscosity of viscoelastic liquids the test fluid must be exposed to a pure elongational flow, in which a cylindrical liquid sample always remains cylindrical and the elongation rate is constant with respect to space and time (Walters, 1975; Petrie, 1979). In some experimental methods the fluid is placed between two disks by surface tension and wall adhesion, forming a liquid bridge (Matta and Tytus, 1990; Sridhar et el., 1991; Berg et al., 1991). The liquid bridge is stretched by increasing the disk distance. While surface-tension forces try to deform the bridge shape to achieve minimum surface area, shearing friction, inertia and flow resistance due to elongational viscosity act against it. The change of the bridge shapes and the velocity field, therefore, depend on the force that is dominant in each case of stretching (Kröger et al., 1992). The initial cylindrical liquid bridge does not stay cylindrical and the local elongation rates within the liquid bridge are not homogeneous. To measure the local differences of the elongation rates within the liquid bridge, flow visualization during stretching experiments with large Newtonian and viscoelastic liquids have been carried out in a Plateau tank.

PURE ELONGATIONAL FLOW

A pure axissymmetric elongational flow (Bird et al.,1977) is a shear free flow with a linear velocity distribution (cylindrical coordinates)

$$v_z = \dot{\epsilon} z, \quad v_r = -\dot{\epsilon} r/2. \tag{1}$$

The non-zero components of the resulting rate-of-strain-tensor are

$$\dot{\gamma}_{zz} = 2\partial v_z/\partial z = 2\dot{\epsilon}, \quad \dot{\gamma}_{rr} = 2\partial v_r/\partial r = -\dot{\epsilon}. \tag{2}$$

As the elongational viscosity η_e is defined as the normal stress difference $\tau_{zz}-\tau_{rr}$ devided by the elongation rate $\dot{\epsilon}$

$$\eta_e = \tau_{zz}-\tau_{rr}/\dot{\epsilon}, \tag{3}$$

the difference $\dot{\gamma}_{zz}-\dot{\gamma}_{rr}$ is of interest. For pure elongational flow $\dot{\gamma}_{zz}-\dot{\gamma}_{rr}$ equals $3\dot{\epsilon}$.

EXPERIMENTAL SETUP

In a Plateau tank the test fluid is placed between two circular plane disks and is surrouded by another fluid of equal density which is immiscible with the test fluid. As gravity is balanced by bouyancy forces the initial liquid bridge shape is cylindrical (initial bridge diameter and length are $2R_0 = L_0 = 50$ mm). The liquid bridge is stretched by moving the upper disk upwards with a constant velocity $u = 8$ mm/s while the lower disk remains at rest. Small particles are added to the liquid and the liquid bridge is illuminated by a light sheet parallel to the bridge axis. Series of photographs with exposure times of 0.5 s are taken to visualize the velocity field.

LIQUIDS

In order to show the different influences of the forces acting in the liquid bridge three Newtonian and three viscoelastic liquids were selected as bridge liquids. The Newtonian liquids were water and two silicon fluids (Dow Corning, 200 Fluid) designated S160 and S3000. As viscoelastic test liquids polyacrylamide copolymer (Stockhausen, PRAESTOL 2500) solutions in double-distilled water of weight concentrations 0.01, 0.3 and 0.9% (designated PAA 0.01%, PAA 0.3% and PAA

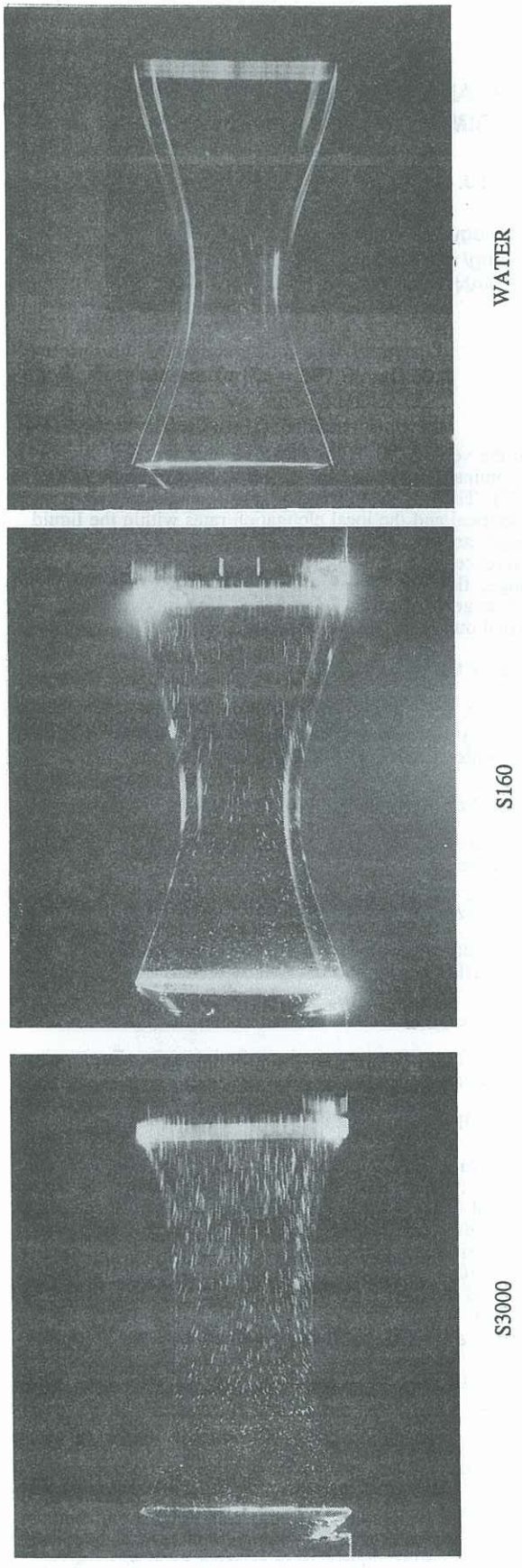

Fig. 1: Photos of stretched liquid bridges (L≈ 90 mm) Newtonian liquids

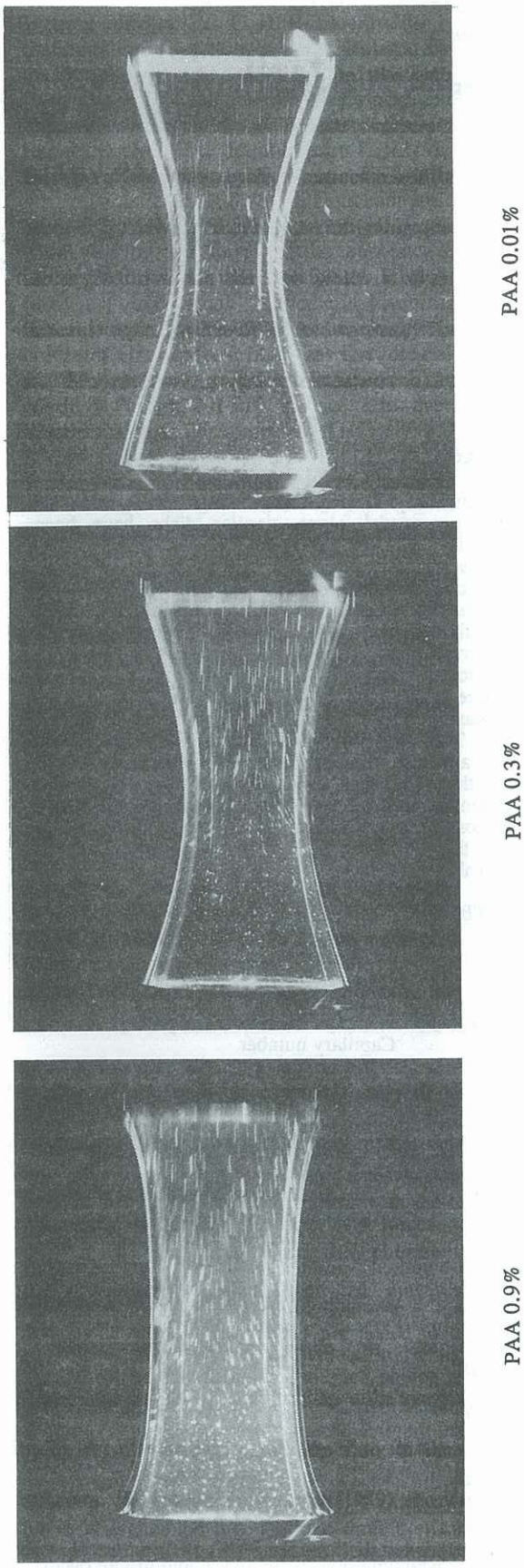

Fig. 1: Photos of stretched liquid bridges (L≈ 90 mm) viscoelastic liquids

0.9%) were used. The PAA solutions show normal stresses and an elongational viscosity that increases with the elongation rate and polymer concentration (Kröger et al., 1992; Ferguson et al., 1990; Jones and Walters, 1989). For all test fluids the (zero) shear viscosities η_S and the Capillary numbers

$$Ca = \eta \cdot u \cdot R_C / (L \cdot \sigma) \qquad (4)$$

are shown in Table I (calculated for an ideal cylinder of length $L = 2\,L_O$ and radius $R_C = R_O\,(L_O/L)^{1/2}$, with L_O= 50 mm, R_O= 25 mm, interface tension σ= 20 mN/m and disk velocity u= 8 mm/s)

Table I: (zero) shear viscosity and Ca of test liquids

liquid	η_S [mPa.s]	1/Ca [-]
water	1	10000
PAA 0.01%	4	4000
S160/PAA 0.3%	160	90
S300/PAA 0.9%	3000	5

EVALUATION PROCEDURE

For each photograph (some samples for L≈90mm are shown in Fig. 1) the liquid bridge contour was approximated by a polynomial function R(z) of 8th order. This function R(z) was used for the optical correction of the light refraction at the bridge surface (see below) and to determine the minimum radius of each bridge shape. In Fig. 2 the minimum radius is ploted versus the bridge length for all examined liquids.

The particle path lines visible on the photos were assumed to represent the local velocities. The corresponding velocity vectors have been digitalized from each photo. After the optical refraction of the Plateau tank wall and the liquid bridge surface was corrected, the velocity field was approximated by functions of the form $v_r(r,z)$ and $v_z(r,z)$ for the velocity components. This approximations have been calculated with Chebyshev polynomials using a least square fit to the measured vectors with the following boundary conditions. The liquid velocities at the disks equal the disk velocities, $v_r(r=0,z)=0$, v_r and v_z are axissymmetric. In general the orders of the Chebyshev polynomials were 3 for v_z in z direction, 4 for v_z in r and v_r in z, and 5 for v_r in r direction. The average difference between the approximation and the measured values of v_r and v_z was calculated and if the difference was larger than half of the measuring error the degrees were increased accordingly. From the velocity approximations $v_r(r,z)$ and $v_z(r,z)$ the velocity and its derivatives with respect to r and z can be determined for each position within the liquid bridge. From that

$$(\dot\gamma_{zz}\text{-}\dot\gamma_{rr})(r,z) = 2\,(\partial v_z/\partial z - \partial v_r/\partial r) \qquad (5)$$

can be calculated.

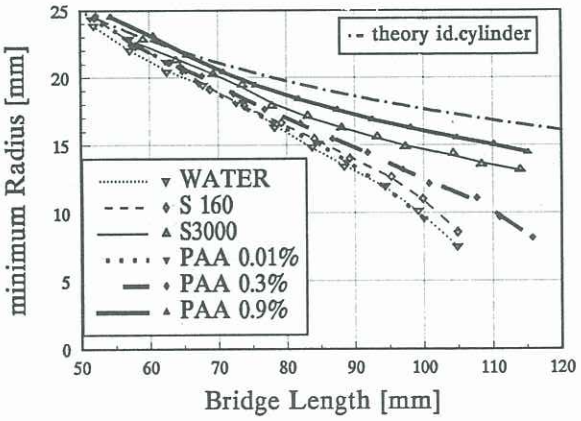

Fig. 2: minimum radius versus bridge length

In order to reduce the large amount of data the following average values have been calculated. The weighted average in the cross section $z=z_0$ was calculated as

$$\{v_z\}(z_0) = \frac{\int_0^{R(z_0)} r\, v_r(r,z_0)\, dr}{\int_0^{R(z_0)} r\, dr} \qquad (6)$$

so that $\{v_z\}(z)$, $\{v_r\}(z)$ and $\{\dot\gamma_{zz}\text{-}\dot\gamma_{rr}\}(z)$ can be calculated for each photo for $0 \le z \le L$. The notations $\{..\}_{max}$ and $\{..\}_{min}$ indicate the maximum and minimum values within the region $0 \le z \le L$. For all liquids plots of $\{v_r\}_{max}$ versus the bridge length are shown in Fig. 3 and the values of $\{\dot\gamma_{zz}\text{-}\dot\gamma_{rr}\}_{max}$ and $\{\dot\gamma_{zz}\text{-}\dot\gamma_{rr}\}_{min}$ are shown in Fig. 4.

In Fig. 1 it can be observed that there are cases in which the liquid flows towards both disks (PAA 0.01%), indicating that $\{v_z\}_{max} > u$ and $\{v_z\}_{min} < 0$. The mean axial velocity relative to the disks was calculated as

$$\{v_z\}_{rel} = (\{v_z\}_{max} - u - \{v_z\}_{min})/2 \qquad (7)$$

for each photo and is shown in Fig. 3 versus the bridge length for all liquids. The overall average $<\dot\gamma_{zz}\text{-}\dot\gamma_{rr}>$ was calculated from

$$<\dot\gamma_{zz} - \dot\gamma_{rr}> = \frac{1}{L}\int_0^L \{\dot\gamma_{zz} - \dot\gamma_{rr}\}(z)\, dz \qquad (8)$$

and is shown in Fig. 4 versus the bridge length for all liquids.

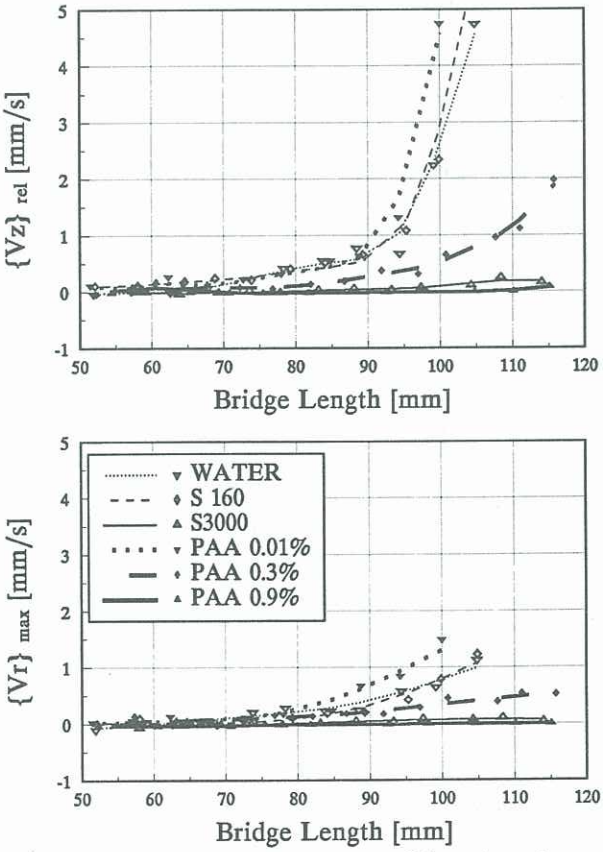

Fig. 3: mean velocity relative to the disks and maximun radial velocity versus bridge length

RESULTS

From Fig. 2 it can be seen, that for all liquids the minimum radius of the liquid bridge, i.e. the most narrow part of the bridge, reduces as the bridge is stretched. While the low viscosity liquid bridges (water and PAA 0.01%) reduce their radius very fast, the high viscosity liquids reduce their radius slower and remain more cylindrical shaped (compare photos in Fig. 1). Newtonian liquid bridges contract faster than viscoelastic bridges which tend to form more cylindrical shapes.

The principal flow field that was observed for all liquids is best illustrated by the photo of the PAA 0.01% flow field in Fig. 1. In the minimum radius region the liquid flows inward towards the bridge axis, and forms a stagnation point. From here the liquid flows towards both disks. If the axial velocity towards the disk is higher than the disk velocity, which is obvious in the PAA 0.01% case, another stagnation point is formed at each disk and the liquid starts flowing outward in front of the disks (vortex kind flow). In Fig. 3 for each photo the maximum axial velocities relative to the disks and the maximum radial velocities away from the bridge axis are ploted versus the bridge length for all liquids. The vortex character can be detected clearly for the low viscosity liquids, but not for the high viscous S3000 and PAA 0.9%.

From the described flow field it is obvious that in the minimum radius region the highest elongation rates occur and that closer to the disks the local elongation rate reduces and can even become negative. In Fig. 4 the overall average $<\dot{\gamma}_{zz}-\dot{\gamma}_{rr}>$ and the maximum $\{\dot{\gamma}_{zz}-\dot{\gamma}_{rr}\}_{max}$ (minimum radius region) and the minimum value $\{\dot{\gamma}_{zz}-\dot{\gamma}_{rr}\}_{min}$ (in front of the disks) are ploted for all liquids versus the bridge length. While the average $<\dot{\gamma}_{zz}-\dot{\gamma}_{rr}>$ is lower than the theoretical value $3\dot{\epsilon}$ the maximum values of $\dot{\gamma}_{zz}-\dot{\gamma}_{rr}$ are significantly higher than $3\dot{\epsilon}$. The differences between $\{\dot{\gamma}_{zz}-\dot{\gamma}_{rr}\}_{max}$ and $\{\dot{\gamma}_{zz}-\dot{\gamma}_{rr}\}_{min}$ indicate the non homogeneous distribution of the local elongation rates within the liquid bridge. This difference increases with a decreasing viscosity of the liquid.

CONCLUSIONS

From the stretching experiments of large Newtonian and viscoelastic liquid bridges the following description of the occuring flow can be given. The liquid bridge is held between two disks by surface tension and wall adhesion. If the bridge is stretched surface tension tries to deform the bridge contour to achieve minimum surface area, while flow resistance due elongational and shear viscosity act against it. A large bridge contraction can be observed for low viscosity liquids in the middle of the bridge, while for high viscous liquids, due to viscous damping, the contraction takes more time and the bridge is more cylindrical like.

In the contraction region a stagnation point can be observed as the liquid flows radially inwards and from here along the axis towards both disks. For low Capillary numbers the flow towards the disks can achieve axial velocities that are larger than the disk velocities, so that a vortex is formed. The liquid now flows radially outward in front of the disks.

It was measured that the local elongation rates in the contraction area are the highest and that in front of the disks negative elongation rates occur. The maximum elongation rates in the middle of the bridge are higher than those calculated from the disk velocity assuming an ideal cylinder. With decreasing Capillary numbers the local elongation rate distribution becomes more non-homogenious.

ACKNOWLEDGEMENT

This work has been supported by the Deutsche Argentur für Raumfahrtangelegenheiten (DARA).

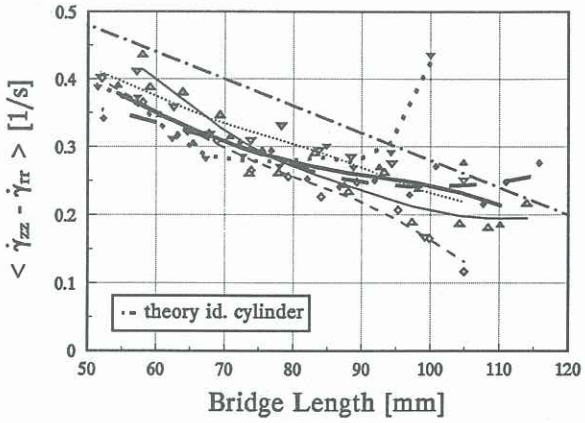

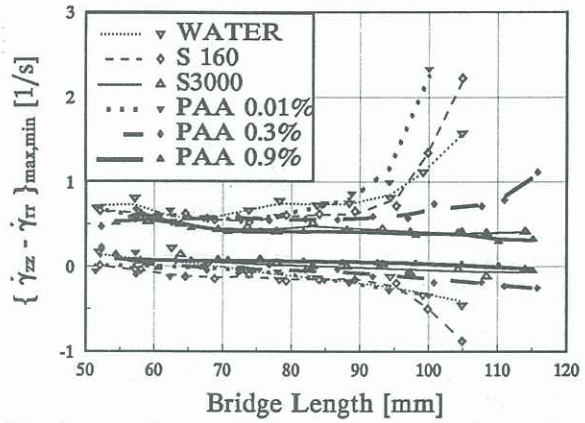

Fig. 4: overall average $<\dot{\gamma}_{zz}-\dot{\gamma}_{rr}>$ and maximum and minimum $\{\dot{\gamma}_{zz}-\dot{\gamma}_{rr}\}_{max,min}$ vs. bridge length

REFERENCES

BERG, S, KRÖGER, R, DELGADO, A, RATH, H-J (1991) Project: Determination of the Elongational Viscosity of Visco-elastic Fluids under Microgravity, FED-Vol. 111, Forum on Microgravity Flows, ASME, 47-51

BIRD, R B, ARMSTRONG, R C, HASSAGER, O (1977) Dynamics of polymeric liquids, Volume 1, Fluid Mechanics, John Wiley & Sons, New York

FERGUSON, J, WALTERS, K, WOLFF, C (1990) Shear and extensional flow of polyacrylamide solutions, Rheol Acta 29, 571-579

JONES, D M, WALTERS, K (1989) The behaviour of polymer solutions in extension-dominated flows, with applications to enhanced oil recovery, Rheol Acta, 28, 482-498

KRÖGER, R, BERG, S, DELGADO, A, RATH, H-J (1992) Stretching behaviour of large polymeric and Newtonian liquid bridges in plateau simulations, J. Non-Newtonian Fluid Mechanics, 45 (to be published)

MATTA, J E, TYTUS, R P (1990) Liquid Stretching Using a Falling Cylinder, J. Non-Newtonian Fluid Mechanics, 35, 215-229

PETRIE, C J S (1979) Elongational Flow, Pitman, London

SRIDHAR, T, TIRTAATMADJA, V, NGUYEN, D A, GUPTA, R K (1991) Measurement of extensional viscosity of polymer solutions, J. Non-Newtonian Fluid Mechanics, 40, 271-280

WALTERS, K (1975) Rheometry, Chapman and Hall, London